View metadata, citation and similar papers at core.ac.uk
brought to you by CORE
provided by Ghent University Academic Bibliography

CONSISTENT JOINT PHOTOMETRIC AND GEOMETRIC IMAGE REGISTRATION

Hiêp Quang Luong, Bart Goossens, Aleksandra Pižurica and Wilfried Philips

Ghent University - TELIN - IPI - IBBT
Sint-Pietersnieuwstraat 41, B-9000 Ghent, Belgium
hiep.luong@telin.ugent.be

ABSTRACT

In this paper, we derive a novel robust image alignment technique that performs joint geometric and photometric registration in the *total least square* sense. The main idea is to use the total least square metrics instead of the ordinary least square metrics, which is commonly used in the literature. While the OLS model indicates that the *target* image may contain noise and the *reference* image should be noise-free, this puts a severe limitation on practical registration problems. By introducing the TLS model, which allows perturbations in both images, we can obtain mutually consistent parameters. Experimental results show that our method is indeed much more consistent and accurate in presence of noise compared to existing registration algorithms.

Index Terms— Photometric and geometric image registration, total least square, orthogonal distance regression

1. INTRODUCTION

General image registration techniques align two (or more) images in the spatial domain. These methods are referred to as *geometric* registration. We refer the interested reader to [1, 2] for comprehensive surveys. In addition, we can also perform image registration/alignment in the range/intensity domain, which is also known as *photometric* registration.

Some registration algorithms are based on the intensity constancy assumption, however in practice, this assumption is not always correct. In an uncontrolled environment, lighting conditions can vary over time (e.g. due to the weather) and intensity variations also arise due to the automatic gain control or automatic white balancing inside the camera. On the other hand, in *high dynamic range* (HDR) imaging, the aperture times and hence the apparent illumination are even changed on purpose.

In the next sections, we briefly discuss the current photometric registration techniques and the total least square formulation, we propose a new approach that jointly performs geometric and photometric registration, we show some experiment results and we end this paper with a conclusion.

2. RELATED WORK IN PHOTOMETRIC REGISTRATION

Photometric registration consists of determining the parameters of the *comparametric equations* (or *intensity mapping functions*) that describe the relationship between the intensity values of the corresponding pixels of two spatially aligned images f and g. Some examples of well-known comparametric models are the linear transformation (also referred to as gain and bias model) and the gamma correction (i.e. raising the pixel values to a power to lighten or darken images). A more detailed overview of comparametric equations and their related camera response functions is given by Mann in [3]. The estimation process of the parameters involves the computation of a *comparagram* (i.e. the joint histogram of the pixel values between the spatially aligned images) and followed by finding a smooth semi-monotonic function (i.e. comparametric equation) that passes through most of the highest bins in the comparagram. In a nutshell, photometric registration comes down to comparametric regression or finding the optimal fit to the comparagram data.

Photometric registration requires the computation of a comparagram, which on its turn requires spatially aligned images. On the other hand, geometric registration techniques are often based on the intensity constancy assumption. This results in a chicken-and-egg problem, which can be solved in three ways: by first using an intensity invariant geometric registration (e.g. based on the gradient constancy) or a spatially invariant photometric registration (e.g. histograms or statistical moments) or by jointly estimating geometric and photometric registration parameters, which is our focus in this paper.

In [4], the authors estimated the linear photometric model using a robust RANSAC algorithm that minimizes the Huber robust loss function. Bartoli performed joint geometric and photometric registration within the inverse compositional gradient-based framework using the ordinary least square metrics [5]. In [6], Aguiar employs a simple two-step iterative algorithm to resolve the registration and exposure parameters. In [7], Grossberg and Nayar determined the camera response function from the intensity mapping functions between several images, which are not spatially aligned. They computed the comparametric parameters directly from cumulative intensity histograms. Candocia approximated the comparametric function and the camera response function by a piecewise linear model [8, 9]. Gevrekci and Gunturk employed a geometric feature point matching algorithm and comparametric regression to perform joint HDR and super-resolution reconstruction [10].

3. THE TOTAL LEAST SQUARE FORMULATION

The standard parametric geometric and comparametric relationship between images f and g is given by the following model:

$$f(\mathbf{x}) = \mathbf{P}(g(\mathbf{G}(\mathbf{x}; \mathbf{p}_\mathrm{G})); \mathbf{p}_\mathrm{P}) + n_f, \tag{1}$$

where $\mathbf{p}_\mathrm{G}$ and $\mathbf{p}_\mathrm{P}$ are the geometric and photometric parameters respectively, $\mathbf{G}$ and $\mathbf{P}$ represent the geometric and photometric models, $\mathbf{x}$ denotes the spatial coordinates and n_f is additive noise. In the *motion-free* case combined with the linear comparametric model, the

comparametric function is simplified to a straight line with gain a_1 and bias a_0 ($\mathbf{p}_\text{P} = [\ a_1 \quad a_0\ ]^\text{T}$):

$$f(\mathbf{x}) = a_1 g(\mathbf{x}) + a_0 + n_f. \tag{2}$$

Note that this comparametric function introduces clipping effects, i.e. saturation of pixel values below 0 and above 255, which implies an important loss of information at very dark and light regions and therefore, these regions should be excluded from further computations. In the presence of additive zero-mean white Gaussian noise, the parameters can be found via *ordinary least squares* (OLS) formulation as employed in e.g. [6, 5, 8]:

$$\begin{aligned}\hat{\mathbf{p}}_\text{P} &= \arg\min_{a_1,a_0} \sum_{\mathbf{x}\in\Omega} d_\text{a}^2 = \arg\min_{a_1,a_0} \sum_{\mathbf{x}\in\Omega} (a_1 g(\mathbf{x}) + a_0 - f(\mathbf{x}))^2 \\ &= \begin{pmatrix} \sum_{\mathbf{x}\in\Omega} g^2(\mathbf{x}) & \sum_{\mathbf{x}\in\Omega} g(\mathbf{x}) \\ \sum_{\mathbf{x}\in\Omega} g(\mathbf{x}) & \sum_{\mathbf{x}\in\Omega} 1 \end{pmatrix}^{-1} \begin{pmatrix} \sum_{\mathbf{x}\in\Omega} g(\mathbf{x}) f(\mathbf{x}) \\ \sum_{\mathbf{x}\in\Omega} f(\mathbf{x}) \end{pmatrix} \end{aligned} \tag{3}$$

where d_a is denoted as the *algebraic distance*.

This OLS model has some serious shortcomings in practice: the estimated parameters are mutual inconsistent, i.e. the inverse forward transformation does not yield the backward transformation and vice versa (both solutions should be symmetric around the bisector of the comparagram). The problem is the incorrect employed model in equation (1), which indicates that image f may contain noise and image g should be noise-free, which is not true in practice.

An improved geometric and photometric registration model specifies that image g can also be subject to perturbations:

$$f(\mathbf{x}) = \mathbf{P}(g(\mathbf{G}(\mathbf{x};\mathbf{p}_\text{G}));\mathbf{p}_\text{P}) + n_f, \tag{4}$$

where n_g is additive noise, commonly from the same probability density function that generates n_f. The solution of this model minimizes the *geometric distance* d_g instead of the algebraic distance d_a. In case of linear comparametric regression (see equation (2)), equation (4) is transformed into a *total least square* (TLS) problem. The solution to the TLS problem is well documented, see e.g. [11, 12].

The linear solution of the problem stated in equation (4) can explicitly be found via the basic TLS algorithm as described in e.g. [12], where $\hat{a}_1$ can be computed via the *singular value decomposition* (SVD) of the following zero-mean shifted augmented matrix:

$$\begin{pmatrix} g(\mathbf{x}_1) - \overline{g} & f(\mathbf{x}_1) - \overline{f} \\ g(\mathbf{x}_2) - \overline{g} & f(\mathbf{x}_2) - \overline{f} \\ \vdots & \vdots \end{pmatrix} = \mathbf{U}\mathbf{\Sigma}\mathbf{V}^\text{T} \tag{5}$$

where $\overline{g}$ and $\overline{f}$ are the mean intensity values of the images g and f respectively. $\mathbf{\Sigma}$ is a 2×2 diagonal matrix with the singular values on the main diagonal and $\mathbf{V}$ is a 2×2 containing the singular vectors. The gain parameter a_1 in the TLS sense is computed by $\hat{a}_1 = -\frac{\mathbf{V}(1,2)}{\mathbf{V}(2,2)}$ on the condition that $\mathbf{V}(2,2)$ is non-zero (or non-singular in general). The bias parameter a_0 can be computed directly by substituting $\hat{a}_1$ back into the following equation: $\hat{a}_0 = \overline{f} - \hat{a}_1\overline{g}$.

Unfortunately, the basic TLS algorithm can only be applied for the linear registration model. Therefore, we use a more general approach in this paper to minimize the geometric distance, which is also referred to as *orthogonal distance regression* [13, 14]:

$$\begin{aligned}\hat{\mathbf{p}}_\text{P} &= \arg\min_{\mathbf{p}_\text{P}} \sum_{\mathbf{x}\in\Omega} d_\text{g}^2 = \arg\min_{\mathbf{p}_\text{P}} \sum_{\mathbf{x}\in\Omega} \|\mathbf{Y}(\mathbf{x}) - \mathbf{Y}'(\mathbf{x};\mathbf{p}_\text{P})\|_2^2 \\ &= -(\mathbf{J}^\text{T}\mathbf{J})^{-1}\mathbf{J}^\text{T}(\mathbf{Y}(\mathbf{x}) - \mathbf{Y}'(\mathbf{x};\mathbf{p}_\text{P})), \end{aligned} \tag{6}$$

where the measurement data $\mathbf{Y}(\mathbf{x})$ (we can interpret this as a point in the comparagram) is given by

$$\mathbf{Y}(\mathbf{x}) = \begin{pmatrix} g(\mathbf{x}) \\ f(\mathbf{x}) \end{pmatrix}. \tag{7}$$

The minimum is found using the iterative Gauss-Newton method. The Jacobian $\mathbf{J}$ in the solution (6) is computed via the chain rule:

$$\begin{aligned}\mathbf{J} &= \sum_{\mathbf{x}\in\Omega} \frac{\partial\|\mathbf{Y}(\mathbf{x}) - \mathbf{Y}'(\mathbf{x};\mathbf{p}_\text{P})\|_2}{\partial\mathbf{p}_\text{P}} \\ &= \sum_{\mathbf{x}\in\Omega} \frac{\left(\mathbf{Y}(\mathbf{x}) - \mathbf{Y}'(\mathbf{x};\mathbf{p}_\text{P})\right)^\text{T}}{\|\mathbf{Y}(\mathbf{x}) - \mathbf{Y}'(\mathbf{x};\mathbf{p}_\text{P})\|_2} \frac{\partial\mathbf{Y}'(\mathbf{x};\mathbf{p}_\text{P})}{\partial\mathbf{p}_\text{P}} \end{aligned} \tag{8}$$

The orthogonal projection $\mathbf{Y}'(\mathbf{x})$ of the measurement data on the regression curve can be found by minimizing the distance between the curve and the measurement data. In some cases, e.g. in the linear photometric registration model, $\mathbf{Y}'(\mathbf{x})$ can be found in a closed-form expression. An additional benefit of this approach is that it also requires less memory compared to the basic TLS algorithm because we do not have to explicitly construct the augmented matrix in equation (5).

4. JOINT TLS IMAGE REGISTRATION

We now derive a novel algorithm that solves the joint photometric linear and geometric affine registration problem in the TLS sense based on orthogonal distance regression. The advantage over the approach of [6, 5] is that our method uses the TLS metrics, which results in more consistent and accurate registration parameters.

The parametric model (4) is transformed into the following (non-linear) assumption:

$$f(x,y) = a_1 g(a_{00} + a_{10}x + a_{01}y, b_{00} + b_{10}x + b_{01}y) + a_0, \tag{9}$$

Like the gradient-based geometric registration algorithms in [15], we iteratively estimate the registration parameters using the incremental updates $\delta\mathbf{p}_\text{G} = [\ \delta a_{00} \quad \delta a_{10} \quad \delta a_{01} \quad \delta b_{00} \quad \delta b_{10} \quad \delta b_{01}\ ]^\text{T}$ and $\delta\mathbf{p}_\text{P} = [\ \delta a_0 \quad \delta a_1\ ]^\text{T}$:

$$\hat{\mathbf{p}}_\text{G}^{(j+1)} = \hat{\mathbf{p}}_\text{G}^{(j)} + \delta\hat{\mathbf{p}}_\text{G}^{(j)} \quad \text{and} \quad \hat{\mathbf{p}}_\text{P}^{(j+1)} = \hat{\mathbf{p}}_\text{P}^{(j)} + \delta\hat{\mathbf{p}}_\text{P}^{(j)}. \tag{10}$$

To find these incremental updates, we approximate the non-linear model by the first order Taylor series expansion:

$$\begin{aligned}\tilde{f}(\mathbf{x}) - \tilde{g}(\mathbf{x}) \approx\ & a_1\nabla_x g(\mathbf{x})\delta a_{00} + a_1 x\nabla_x g(\mathbf{x})\delta a_{10} \\ & + a_1 y\nabla_x g(\mathbf{x})\delta a_{01} + a_1\nabla_y g(\mathbf{x})\delta b_{00} \\ & + a_1 x\nabla_y g(\mathbf{x})\delta b_{10} + a_1 y\nabla_y g(\mathbf{x})\delta b_{01} \\ & + g(\mathbf{x})\delta a_1 + \delta a_0, \end{aligned} \tag{11}$$

where we iteratively perform the inverse geometric registration and the forward photometric registration by transforming $\tilde{f}(\mathbf{x}) = f\left(\mathbf{G}^{-1}\left(\mathbf{x};\hat{\mathbf{p}}_\text{G}^{(j)}\right)\right)$ and $\tilde{g}(\mathbf{x}) = \mathbf{P}\left(g(\mathbf{x});\hat{\mathbf{p}}_\text{P}^{(j)}\right)$ respectively.

The estimation of the registration parameters in the linearized model can be interpreted as a regression problem that fits the parameters to a hyperplane, given by the following implicit function (where we have simplified some notations[1]):

$$h(\mathbf{Y},\boldsymbol{\delta}) = \sum_{i=0}^{6} Y_i\delta_i + \delta_7 - Y_7 = 0. \tag{12}$$

[1] $\delta_0 = \delta a_{00}$, $\delta_1 = \delta a_{10}$, $\delta_2 = \delta a_{01}$, $\delta_3 = \delta b_{00}$, $\delta_4 = \delta b_{10}$, $\delta_5 = \delta b_{01}$, $\delta_6 = \delta a_1$ and $\delta_7 = \delta a_0$.

Similarly to the orthogonal distance regression formulation in equation (6), the measurement data of this hyperplane is given by

$$\mathbf{Y}(\mathbf{x}) = \begin{pmatrix} Y_0(\mathbf{x}) \\ Y_1(\mathbf{x}) \\ Y_2(\mathbf{x}) \\ Y_3(\mathbf{x}) \\ Y_4(\mathbf{x}) \\ Y_5(\mathbf{x}) \\ Y_6(\mathbf{x}) \\ Y_7(\mathbf{x}) \end{pmatrix} = \begin{pmatrix} a_1 \nabla_x g(\mathbf{x}) \\ a_1 x \nabla_x g(\mathbf{x}) \\ a_1 y \nabla_x g(\mathbf{x}) \\ a_1 \nabla_y g(\mathbf{x}) \\ a_1 x \nabla_y g(\mathbf{x}) \\ a_1 y \nabla_y g(\mathbf{x}) \\ g(\mathbf{x}) \\ \tilde{f}(\mathbf{x}) - \tilde{g}(\mathbf{x}) \end{pmatrix}. \quad (13)$$

The orthogonal projection $\mathbf{Y}'$ on the hyperplane is denoted by the following system of symmetric line equations:

$$\begin{cases} \frac{\mathbf{Y}'_0 - \mathbf{Y}_0}{\delta_0} = \frac{\mathbf{Y}'_1 - \mathbf{Y}_1}{\delta_1} = \ldots = -\mathbf{Y}'_7 + \mathbf{Y}_7 \\ h(\mathbf{Y}'_l, \boldsymbol{\delta}) = 0 \end{cases} \quad (14)$$

By solving this system, we obtain the closed-form expression for $\mathbf{Y}'$, which is given by

$$\mathbf{Y}'(\mathbf{x}, \boldsymbol{\delta}) = \begin{pmatrix} Y_0(\mathbf{x}) - \delta_0 \frac{\xi(\mathbf{x}, \boldsymbol{\delta})}{\upsilon(\boldsymbol{\delta})} \\ \vdots \\ Y_6(\mathbf{x}) - \delta_6 \frac{\xi(\mathbf{x}, \boldsymbol{\delta})}{\upsilon(\boldsymbol{\delta})} \\ Y_7(\mathbf{x}) + \frac{\xi(\mathbf{x}, \boldsymbol{\delta})}{\upsilon(\boldsymbol{\delta})} \end{pmatrix}, \quad (15)$$

where we employ $\xi(\mathbf{x}, \boldsymbol{\delta})$ and $\upsilon(\boldsymbol{\delta})$ as the shorthand notations for

$$\xi(\mathbf{x}, \boldsymbol{\delta}) = \delta_7 - Y_7(\mathbf{x}) + \sum_{i=0}^{6} Y_i(\mathbf{x}) \delta_i \quad \text{and} \quad \sum_{i=0}^{6} \delta_i^2 + 1. \quad (16)$$

In order to compute the Jacobian $\mathbf{J}$ in equation (8), we have to obtain the partial derivatives of $\mathbf{Y}'$ to $\boldsymbol{\delta}$. This is given for the case of δ_0 (the cases from δ_1 to δ_6 are similar):

$$\frac{\partial \mathbf{Y}'(\mathbf{x}, \boldsymbol{\delta})}{\partial \delta_0} = \begin{pmatrix} \frac{2\delta_0^2}{\upsilon(\boldsymbol{\delta})} \frac{\xi(\mathbf{x}, \boldsymbol{\delta})}{\upsilon(\boldsymbol{\delta})} - \frac{\delta_0 Y_0(\mathbf{x})}{\upsilon(\boldsymbol{\delta})} - \frac{\xi(\mathbf{x}, \boldsymbol{\delta})}{\upsilon(\boldsymbol{\delta})} \\ \frac{2\delta_0 \delta_1}{\upsilon(\boldsymbol{\delta})} \frac{\xi(\mathbf{x}, \boldsymbol{\delta})}{\upsilon(\boldsymbol{\delta})} - \frac{\delta_1 Y_0(\mathbf{x})}{\upsilon(\boldsymbol{\delta})} \\ \vdots \\ \frac{2\delta_0 \delta_6}{\upsilon(\boldsymbol{\delta})} \frac{\xi(\mathbf{x}, \boldsymbol{\delta})}{\upsilon(\boldsymbol{\delta})} - \frac{\delta_6 Y_0(\mathbf{x})}{\upsilon(\boldsymbol{\delta})} \\ \frac{-2\delta_0}{\upsilon(\boldsymbol{\delta})} \frac{\xi(\mathbf{x}, \boldsymbol{\delta})}{\upsilon(\boldsymbol{\delta})} + \frac{Y_0(\mathbf{x})}{\upsilon(\boldsymbol{\delta})} \end{pmatrix}, \quad (17)$$

and δ_7:

$$\frac{\partial \mathbf{Y}'(\mathbf{x}, \boldsymbol{\delta})}{\partial \delta_7} = \begin{pmatrix} \frac{-\delta_0}{\upsilon(\boldsymbol{\delta})} \\ \vdots \\ \frac{-\delta_6}{\upsilon(\boldsymbol{\delta})} \\ \frac{1}{\upsilon(\boldsymbol{\delta})} \end{pmatrix}. \quad (18)$$

The difference vector $\mathbf{Y}(\mathbf{x}) - \mathbf{Y}'(\mathbf{x}, \boldsymbol{\delta})$ and its l_2-norm become

$$\mathbf{Y}(\mathbf{x}) - \mathbf{Y}'(\mathbf{x}, \boldsymbol{\delta}) = \begin{pmatrix} \delta_0 \frac{\xi(\mathbf{x}, \boldsymbol{\delta})}{\upsilon(\boldsymbol{\delta})} \\ \vdots \\ \delta_6 \frac{\xi(\mathbf{x}, \boldsymbol{\delta})}{\upsilon(\boldsymbol{\delta})} \\ -\frac{\xi(\mathbf{x}, \boldsymbol{\delta})}{\upsilon(\boldsymbol{\delta})} \end{pmatrix}, \quad (19)$$

$$\|\mathbf{Y}(\mathbf{x}) - \mathbf{Y}'(\mathbf{x}, \boldsymbol{\delta})\|_2 = \frac{|\xi(\mathbf{x}, \boldsymbol{\delta})|}{\sqrt{\upsilon(\boldsymbol{\delta})}}. \quad (20)$$

The Jacobian matrix $\mathbf{J}$ can be simplified by substituting expressions (17)- (20) into equation (8):

$$\mathbf{J}(\boldsymbol{\delta}) = \begin{pmatrix} \sum_{\mathbf{x} \in \Omega} \operatorname{sign}(\xi(\mathbf{x}, \boldsymbol{\delta})) \frac{Y_0(\mathbf{x}) \upsilon(\boldsymbol{\delta}) - \delta_0 \xi(\mathbf{x}, \boldsymbol{\delta})}{\upsilon(\boldsymbol{\delta})^{3/2}} \\ \vdots \\ \sum_{\mathbf{x} \in \Omega} \operatorname{sign}(\xi(\mathbf{x}, \boldsymbol{\delta})) \frac{Y_6(\mathbf{x}) \upsilon(\boldsymbol{\delta}) - \delta_6 \xi(\mathbf{x}, \boldsymbol{\delta})}{\upsilon(\boldsymbol{\delta})^{3/2}} \\ \sum_{\mathbf{x} \in \Omega} \frac{\operatorname{sign}(\xi(\mathbf{x}, \boldsymbol{\delta}))}{\sqrt{\upsilon(\boldsymbol{\delta})}} \end{pmatrix}. \quad (21)$$

The incremental updates $\delta \mathbf{p}_{\mathrm{G}}$ and $\delta \mathbf{p}_{\mathrm{P}}$ are computed by substituting the expressions (13), (15) and (21) into the orthogonal distance regression solution given by equation (6). These updates iteratively improve the current registration parameters as given by equation (10). To avoid local minima and to reduce computation time, we used a coarse-to-fine Gaussian pyramid multi-resolution framework as in [16]. At each level, the computed transformations are served as initial guesses to the next level. Note that derivations for other transformation models can be deducted in a similar way.

5. EXPERIMENTAL RESULTS

In a controlled experiment, we perform a quantitative evaluation of the joint geometric and photometric registration algorithms according to the affine/linear model (9). We simulate 10 degraded 512×512 image pairs (the so-called reference and target images) from 10 random test images by successively applying (i) a Tukey windowing function (to prevent the influence of non-overlapping regions due to the spatial deformations [17]), (ii) random photometric linear (with gain parameters within $[0.8, 1.2]$ and bias parameters within $[-25, 25]$) and geometric affine transformations (the maximum pixel displacement is 32), (iii) decimation (via averaging of 2×2 blocks) and (iv) adding zero-mean white Gaussian noise to both the reference and the target image (with standard deviation σ_{n}). The images are then (v) clipped at $[0, 255]$. This procedure is repeated 26 times for each noise level ($0 \leq \sigma_{\mathrm{n}} \leq 25$).

We compare the proposed TLS solution as described in Section 4 to its OLS counterpart (via the Gauss-Newton optimization, a similar derivation for geometric registration is given in [15]) and the joint geometric linear and photometric affine registration algorithm of Bartoli [5], which operates in an inverse compositional gradient-based framework using the ordinary least square metrics.

Only our TLS algorithm was able to produce mutually consistent photometric registration parameters in presence of noise (i.e. the inverse forward photometric transformation is approximately the same as the backward photometric transformation and vice versa, see also Section 3). The average RMSE accuracy of all registration parameters is plotted in Figure 1 in function of the noise standard deviation. The proposed TLS solution clearly produces more accurate parameters as the amount of noise is increasing (note that if clipping at $[0, 255]$ was not applied, the OLS and Bartoli (photometric) results are even far more worse).

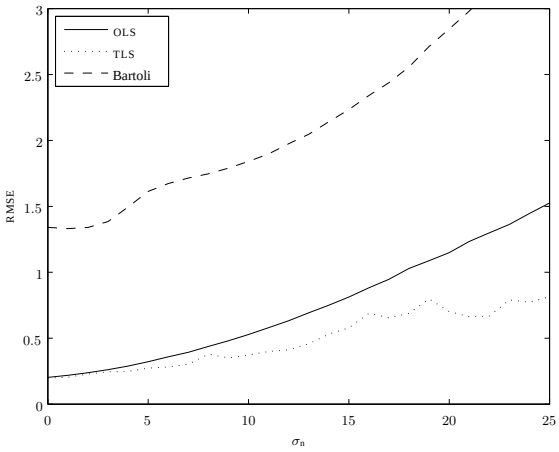

Fig. 1. Average RMSE accuracy of all registration parameters in function of additive zero-mean white Gaussian noise standard deviation σ_n.

6. CONCLUSION

For the photometric and joint geometric/photometric registration problem, we have introduced the use of the total least square framework in the proposed registration algorithms. Our registration method produces more accurate and consistent registration parameters compared to the methods that use the ordinary least square approach, which are commonly employed in the literature. This common model puts severe limitations to practical applications because it assumes that the reference image is noise-free. Conversely, our proposed model also allows perturbations to the reference image. We have derived our registration algorithm within the orthogonal distance regression approach, which has mainly two advantages compared to the basic TLS algorithm (computed via the SVD of the augmented matrix): it is not limited to linear registration models and it has a smaller memory footprint.

7. REFERENCES

[1] L.G. Brown, "A survey of image registration techniques," *ACM Computing Surveys*, vol. 24, pp. 326–376, 1992.

[2] B. Zitová and J. Flusser, "Image registration methods: a survey," *Image and Vision Computing*, vol. 21, pp. 977–1000, 2003.

[3] S. Mann, "Comparametric equations with practical applications in quantigraphic image processing," *IEEE Transactions on Image Processing*, vol. 9, no. 8, pp. 1389–1406, Aug. 2000.

[4] D.P. Capel and A. Zisserman, "Computer vision applied to super resolution," *IEEE Signal Processing Magazine*, vol. 20, no. 3, pp. 75–86, May 2003.

[5] A. Bartoli, "Groupwise geometric and photometric direct image registration," *IEEE Transactions on Pattern Analysis and Machine Intelligence*, vol. 30, no. 12, pp. 2098–2108, Dec. 2008.

[6] P.M.Q. Aguiar, "Unsupervised simultaneous registration and exposure correction," in *Proceedings of IEEE International Conference on Image Processing (ICIP)*, 2006, pp. 361–364.

[7] M.D. Grossberg and S.K. Nayar, "Determining the camera response from images: What is knowable?," *IEEE Transactions on Pattern Analysis and Machine Intelligence*, vol. 25, no. 11, pp. 1455–1467, Nov. 2003.

[8] F.M. Candocia, "Jointly registering images in domain and range by piecewise linear comparametric analysis," *IEEE Transactions on Image Processing*, vol. 12, no. 4, pp. 409–419, Apr. 2003.

[9] F.M. Candocia and D.A. Mandarino, "A semiparametric model for accurate camera response function modeling and exposure estimation from comparametric data," *IEEE Transactions on Image Processing*, vol. 14, no. 8, pp. 1138–1150, Aug. 2005.

[10] M. Gevrekci and B.K. Gunturk, "Superresolution under photometric diversity of images," *EURASIP Journal on Advances in Signal Processing*, vol. 2007, pp. 1–12, 2007, Article ID 36076.

[11] G. Golub and C. Van Loan, "An analysis of the total least squares problem," *SIAM Journal of Numerical Analysis*, vol. 17, pp. 883–893, 1980.

[12] I. Markovsky and S. Van Huffel, "Overview of total least-squares methods," *Signal Processing*, vol. 87, pp. 2283–2302, 2007.

[13] S. Sullivan, L. Sandford, and J. Ponce, "Using geometric distance fits for 3-D object modeling and recognition," *IEEE Transactions on Pattern Analysis and Machine Intelligence*, vol. 16, no. 12, pp. 1183–1196, Dec. 1994.

[14] S.J. Ahn, W. Rauh, H.S. Cho, and H.-J. Warnecke, "Orthogonal distance fitting of implicit curve and surfaces," *IEEE Transactions on Pattern Analysis and Machine Intelligence*, vol. 24, no. 5, pp. 620–638, May 2002.

[15] S. Baker and I. Matthews, "Lucas-Kanade 20 years on: a unifying framework," *International Journal of Computer Vision*, vol. 56, no. 3, pp. 221–255, 2004.

[16] J.R. Bergen, P. Anandan, K.J. Hanna, and R. Hingorani, "Hierarchical model-based motion estimation," in *Proceedings of the Second European Conference on Computer Vision (ECCV)*, 1992, pp. 237–252.

[17] P. Vandewalle, *Super-Resolution From Unregistered Aliased Images*, Ph.D. thesis, École Polytechnique Fédérale de Lausanne (EPFL), 2006.